JBC RESEARCH ARTICLE

Residues E53, L55, H59, and G70 of the cellular receptor protein Tva mediate cell binding and entry of the novel subgroup K avian leukosis virus

Received for publication, July 15, 2022, and in revised form, January 14, 2023 Published, Papers in Press, January 28, 2023,
https://doi.org/10.1016/j.jbc.2023.102962

Xinyi Li[1,‡], Yuntong Chen[1,‡], Mengmeng Yu[1], Suyan Wang[1], Peng Liu[1], Lingzhai Meng[1], Ru Guo[1], Xiaoyan Feng[1], Mingxue Hu[1], Tana He[1], Xiaole Qi[1], Kai Li[1], Li Gao[1], Yanping Zhang[1], Changjun Liu[1], Hongyu Cui[1], Xiaomei Wang[1,2], and Yulong Gao[1,*]

From the [1]Avian Immunosuppressive Diseases Division, State Key Laboratory of Veterinary Biotechnology, Harbin Veterinary Research Institute, The Chinese Academy of Agricultural Sciences, Harbin, PR China; [2]Jiangsu Co-Innovation Center for the Prevention and Control of Important Animal Infectious Disease and Zoonose, Yangzhou University, Yangzhou, PR China

Reviewed by members of the JBC Editorial Board. Edited by Karin Musier-Forsyth

Subgroup K avian leukosis virus (ALV-K) is a novel subgroup of ALV isolated from Chinese native chickens. As for a retrovirus, the interaction between its envelope protein and cellular receptor is a crucial step in ALV-K infection. Tva, a protein previously determined to be associated with vitamin B_{12}/cobalamin uptake, has been identified as the receptor of ALV-K. However, the molecular mechanism underlying the interaction between Tva and the envelope protein of ALV-K remains unclear. In this study, we identified the C-terminal loop of the LDL-A module of Tva as the minimal functional domain that directly interacts with gp85, the surface component of the ALV-K envelope protein. Further point-mutation analysis revealed that E53, L55, H59, and G70, which are exposed on the surface of Tva and are spatially adjacent, are key residues for the binding of Tva and gp85 and facilitate the entry of ALV-K. Homology modeling analysis indicated that the substitution of these four residues did not significantly impact the Tva structure but impaired the interaction between Tva and gp85 of ALV-K. Importantly, the gene-edited DF-1 cell line with precisely substituted E53, L55, H59, and G70 was completely resistant to ALV-K infection and did not affect vitamin B_{12}/cobalamin uptake. Collectively, these findings not only contribute to a better understanding of the mechanism of ALV-K entry into host cells but also provide an ideal gene-editing target for antiviral study.

Avian leukosis viruses (ALVs) belong to a class of alpharetrovirus that is responsible for various tumor diseases. ALVs are divided into 11 subgroups (A–K) according to their host range, envelope (Env) antigenicity, genomic characteristics, viral interference test, serological cross-reaction, etc. Among them, ALV-K is an emerging ALV subgroup isolated and identified in China in 2012 (1), which mainly induces immune system damage, gliomas, and growth retardation (2, 3). Furthermore, many recombinant or mutant events have been identified in ALV-K isolates in recent years, making them more pathogenic and transmissible (4–6). All these factors bring new challenges to the prevention and control of avian leukosis in China. Binding to cell receptors and entering the cells is a crucial step in successfully infection of host cells with ALV. Therefore, elucidating the mechanism of ALV-K entry into cells is crucial for the development of novel prevention and control strategies.

As a retrovirus, ALV requires interactions between the viral Env and cellular receptor proteins for entering a host cell. In ALV, Env is a heterodimer composed of surface (gp85) and a transmembrane (gp37) protein. For ALV, the initial interaction of gp85 with special cell receptors triggers structural rearrangements in gp37 and subsequent steps in the viral infection of host cells (7, 8). Therefore, analysis of the interaction between gp85 and cell receptors could provide a deeper understanding of the mechanisms of ALV entry into cells. Like other simple retroviruses, including murine leukemia viruses (9) and equine infectious anemia viruses (10), ALVs use only one functional receptor to enter cells. However, different subgroups of ALV utilize different cell receptors to enter host cells. ALV-A uses Tva proteins as its receptors (11, 12); ALV-B, ALV-D, and ALV-E use Tvb proteins to enter host cells (13, 14); Tvc proteins are the receptors of ALV-C (15, 16), and ALV-J uses chNHE1 proteins as its receptors (17, 18). Recently, Tva was identified as the cell receptor of ALV-K (19, 20).

Although different subgroups of the same retrovirus may utilize the same receptor to enter host cells, they may interact with different functional domains of the receptor. For example, both feline leukemia virus subgroup B (FeLV-B) and T-cell-tropic FeLV (FeLV-T) use phosphate transport proteins (Pit1) as receptors to enter host cells. The residues 550 to 558 and loop 2 in Pit1 are the crucial functional domains for FeLV-T entry (21), whereas FeLV-B uses residues 546 to 558 only to enter cells (22). In addition, the key residues for the interaction of Tvb with ALV-B/-D are L36, Q37, L41, and Y42 (23). However, Y67, N72, and D73 are important determinants of the interaction of Tvb with ALV-E (24). Thus, although

‡ These authors contributed equally to this work.
* For correspondence: Yulong Gao, gaoyulong@caas.cn.

© 2023 THE AUTHORS. Published by Elsevier Inc on behalf of American Society for Biochemistry and Molecular Biology. This is an open access article under the CC BY-NC-ND license (http://creativecommons.org/licenses/by-nc-nd/4.0/).

ALV-K shares its cellular receptor with ALV-A, it is still not clear whether the mechanism by which ALV-K utilizes Tva to enter cells is similar to that employed by ALV-A.

Tva proteins are related to low-density lipoprotein receptors, which consist of an amino-terminal extracellular domain of 83 residues and transmembrane and cytoplasmic tail regions of 23 and 32 amino acids, respectively (11). Its extracellular domain contains one cysteine-rich region (LDL-A) located between residues 11 and 50 with three disulphide bonds between the six cysteines. Initial studies have identified LDL-A to be necessary and sufficient for Tva to mediate ALV-K entry into host cells (19, 25). Moreover, the LDL-A domain has been reported as the key functional domain of the receptors of various alphaviruses (26). Therefore, exploring the mechanism of interaction between the LDL-A domain and ALV-K is of great significance for an in-depth understanding of the receptor function of Tva.

To elucidate the mechanism of ALV-K entry, we explored the molecular details of the interaction between ALV-K and its receptors. We employed complementary mapping strategies to identify the key domains responsible for Tva receptor function. We found that the C-terminal (CT) loop of the LDL-A module of Tva is responsible for binding with ALV-K gp85. Furthermore, we demonstrate that residues E53, L55, H59, and G70 are the key functional residues responsible for mediating the ALV-K entry into host cells. We further determined that the substitution of these residues did not affect the Tva structure but resulted in impaired interaction between Tva and ALV-K gp85. More importantly, DF-1 cells with substituted E53, L55, H59, and G70 of Tva could completely resist the ALV-K entry.

Results

The CT loop of the LDL-A module is the major functional domain of the Tva receptor for ALV-K

Tva contains an LDL-A module that is highly homologous to huLDLR4. The LDL-A module is a cysteine-rich domain that relies on six cysteines to form two loop domains: the N-terminal (NT) and CT loops (Fig. 1*A*). To determine the key functional domain of Tva that mediates ALV-K entry into host cells, we adopted domain-exchange strategies between Tva and huLDLR4 LDL-A modules. Based on WTTva backbone, the NT or CT loop was replaced with the corresponding segment of huLDLR4 to construct two chimeric plasmids (ch-hu NT and ch-hu CT) (Fig. 1*A*). Western blot analysis results showed that all the chimeric plasmids are well expressed (Fig. 1*B*) further, confocal assays' results showed that Tva proteins and their variants are localized to the surface of transfected cells (Fig. 1*C*).

The plasmids were then transfected into *Tva* knockout DF-1 (DF-1-TvaKO) cells, a nonpermissive cell line for ALV-K (19). After 24 h, the transfected cells were infected with ALV-K recombinant fluorescent virus (RCAS(K)GFP) for the virus entry assay. The results showed that, compared with the WTTva-transfected group, ch-hu NT could effectively mediate RCAS(K)GFP entry (Fig. 1*D*), showing a relative GFP-positive rate of over 88% (Fig. 1*E*). However, ch-hu CT- and huLDLR4-transfected groups could not be infected by RCAS(K)GFP (Fig. 1*D*), and their relative GFP-positive rates were less than 5% (Fig. 1*E*). These results suggest that the CT loop is the key functional domain of Tva that mediates the ALV-K entry into host cells.

Co-immunoprecipitation (Co-IP) assays were performed to verify the above results. First, ch-hu NT and ch-hu CT plasmids were engineered to replace transmembrane domains with Fc tags for soluble expression. The gp85-encoding plasmid was cotransfected with either ch-hu NT or ch-hu CT plasmids into 293T cells. Co-IP assays revealed that WTTva and ch-hu NT could form a specific complex with gp85, whereas huLDLR4 and ch-hu CT did not (Fig. 1*F*). The protein-cell binding assay (18, 27) was performed to verify the Co-IP results. The plasmids (WTTva, huLDLR4, ch-hu NT, and ch-hu CT) were transfected into 293T cells, and the cells were harvested at 24 h post-transfection for the assay. The results showed that, compared with the WTTva-transfected group, the relative gp85-binding capacity of ch-hu NT was more than 90%, whereas that of huLDLR4 and ch-hu CT was less than 10% (Fig. 1*G*). These results suggest that the CT loop is the key functional domain of Tva involved in interaction with gp85.

To further identify the minimal functional domain of Tva mediating ALV-K entry into host cells, the CT loop of the LDL-A module Tva was divided into three segments (L1, L2, and L3) using cysteines as nodes (Fig. 2*A*), which were replaced with corresponding segments of huLDLR4 to construct three chimeric plasmids (ch-hu L1, ch-hu L2, and ch-hu L3) (Fig. 2*A*). The results of the virus entry assay showed that, in comparision with the WTTva-transfected group, the ability of ch-hu L1, ch-hu L2, and ch-hu L3 to mediate RCAS(K)GFP entry into DF-1-TvaKO cells was significantly decreased (Fig. 2*B*), and the relative GFP-positive rate was only 42% to 56% (Fig. 2*C*). Co-IP results showed that ch-hu L1, ch-hu L2, and ch-hu L3 interacted with gp85, but the interaction between them and gp85 was weaker than that of Tva (Fig. 2*D*).

Altogether, these findings indicate that the C-terminus of Tva is the minimal domain responsible for gp85-binding and for mediating ALV-K entry into host cells.

Residues E53, L55, H59, and G70 are key amino acids of the LDL-A module of Tva mediating the virus entry

Nine amino acids in the CT loop of the LDL-A module of Tva were different from those of huLDLR4. To map the key residues responsible for Tva receptor function, we constructed nine chimeric plasmids (Y50I, L52Q, E53L, L55A, G58N, H59D, D63E, R66S, and G70PQR) in which these residues were replaced with the corresponding residues of huLDLR4 (Fig. 3*A*). All plasmids were transfected into DF-1-TvaKO cells for the virus entry assay. The results showed that, compared with the WTTva-transfected group, the ability of E53L, L55A, H59D, and G70PQR to mediate RCAS(K)GFP entry into DF-1-TvaKO cells was significantly decreased (Fig. 3*B*), showing a 40% to 65% relative GFP-positive rate

ASBMB

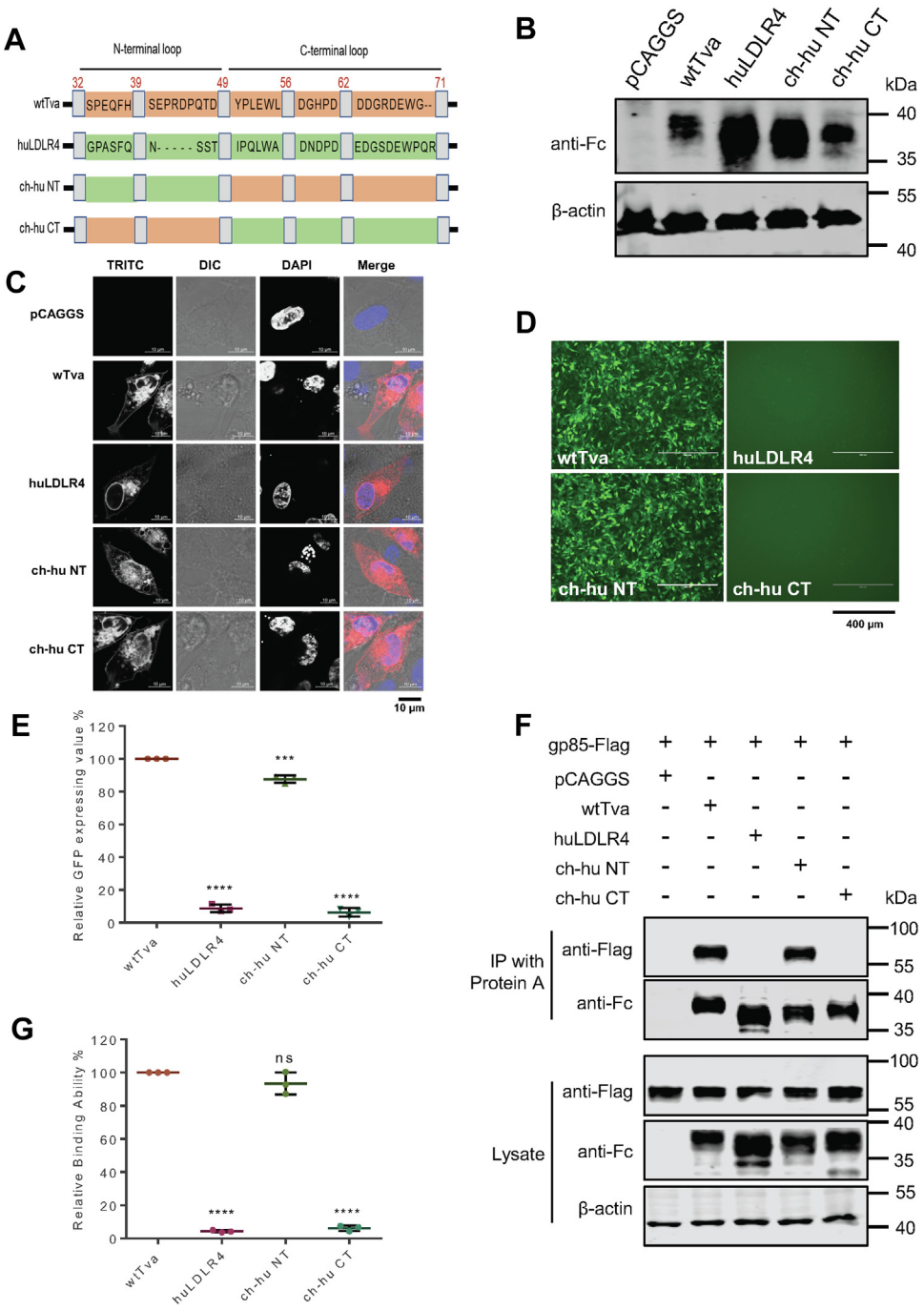

Figure 1. The CT loop of the LDL-A module in Tva is the major receptor functional domain for ALV-K. *A*, schematic representation of ch-hu NT and ch-hu CT construction strategy. *Orange*, WTTva segments; *green*, huLDLR4 segments; *gray*, cystines. *B*, whole cell lysates from transfected cells expressing pCAGGS, WTTva, huLDLR4, ch-hu NT, and ch-hu CT detected by Western blot. *C*, the expression of pCAGGS, WTTva, huLDLR4, ch-hu NT, and ch-hu CT on cell membrane observed by using laser confocal microscope. *D*, the entry of RCAS(K)GFP recombinant virus into DF-1-*Tva*KO cells expressing ch-hu NT or ch-hu CT. The fluorescence in WTTva or huLDLR4 transfected cells was used as a positive control (PC) and negative control (NC). The scale bar represents 400 μm. *E*, virus entry levels of ch-hu NT and ch-hu CT expressing cells were detected by flow cytometry. The virus entry-level of WTTva transfected cells was set to 100%, and the values for chimeric Tva receptors were calculated as their proportion. *F*, interaction of different receptors with gp85 was verified by Co-IP assay. WTTva was used as PC; huLDLR4 was used as NC. *G*, the gp85-binding ability of different receptors expressed on the surface of transfected 293T cells was detected by the protein-cell binding assay. The binding ability of WTTva was set to 100%, and the values of other chimeric receptors were calculated as its proportion. Three independent experiments were performed, and data are shown as means ± SD for triplicates from a representative experiment. $^{**}p < 0.01$; $^{****}p < 0.0001$; ns, no significant difference. ALV, avian leukosis virus; CT, C-terminal; Co-IP, Co-immunoprecipitation; NT, N-terminal.

(Fig. 3*C*). In contrast, Y50I, L52Q, G58N, D63E, and R66S could efficiently mediate RCAS(K)GFP entry into DF-1-TvaKO cells (Fig. 3*B*), and their relative GFP-positive rate was over 85% (Fig. 3*C*). These findings indicate that E53, L55, H59, and G70 are important residues of Tva that mediate ALV-K entry into host cells.

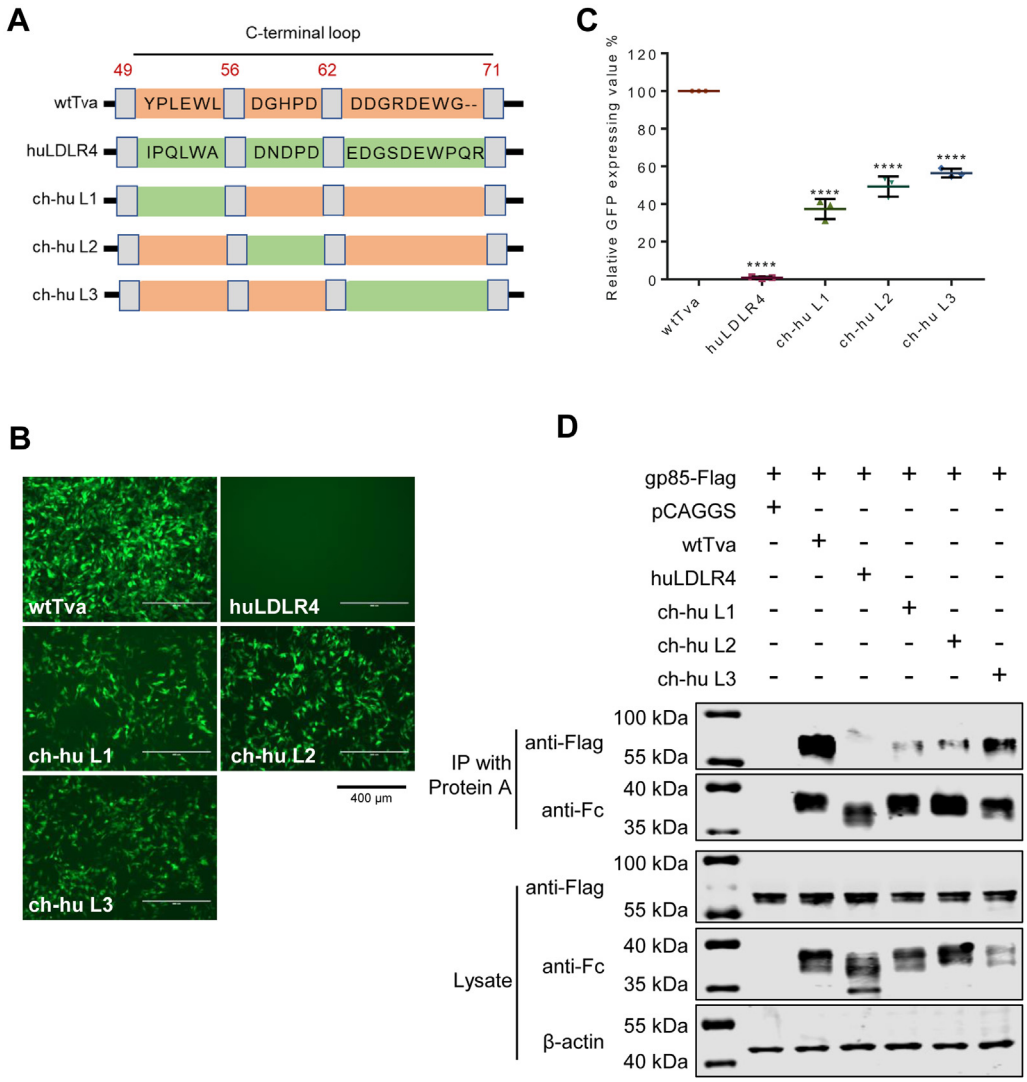

Figure 2. All the three segments in the CT of Tva were involved in mediating virus entry and interaction with gp85. *A*, schematic representation of ch-hu L1, ch-hu L2, and ch-hu L3 construction strategy. *Orange*, WTTva segments; *green*, huLDLR4 segments; *gray*, cystines. *B*, RCAS(K)GFP recombinant virus was entered into DF-1-*Tva*KO cells expressing ch-hu L1, ch-hu L2, or ch-hu L3. The fluorescence in WTTva and huLDLR4 transfected cells was used as PC and NC, respectively. The scale bar represents 400 μm. *C*, virus entry levels of ch-hu L1, ch-hu L2, and ch-hu L3 expressing cells were detected by flow cytometry. The virus entry-level of WTTva-transfected cells was set to 100%, and the values for chimeric Tva receptors were calculated as their proportion. *D*, interaction of ch-hu L1, ch-hu L2, or ch-hu L3 with gp85 was verified by Co-IP assay. Three independent experiments were performed, and data are shown as means ± SD for triplicates from a representative experiment. ****$p < 0.0001$. CT, C-terminal; Co-IP, Co-immunoprecipitation; NT, N-terminal; NC, negative control; PC, positive control.

Residues E53, L55, H59, and G70 directly interact with gp85 protein

To verify the effects of the four identified amino acids on the Tva receptor function, we constructed a chimeric Tva plasmid (rTva), in which E53, L55, H59, and G70 were simultaneously replaced with the corresponding residues of huLDLR4. First, the virus entry assay indicated that rTva completely lost the ability to mediate RCAS(K)GFP entry into host cells (Fig. 4*A*), showing a relative GFP-positive rate of less than 0.5% (Fig. 4*B*). Co-IP assays showed that the soluble form of rTva did not form a special complex with gp85 (Fig. 4*C*). Moreover, the results of the protein-cell binding assay further showed that rTva could not bind with gp85 (Fig. 4*D*). These findings indicate that E53, L55, H59, and G70 are key residues of Tva that mediate ALV-K entry into host cells and bind with gp85.

To further analyze the molecular details of the binding of Tva with gp85, the structures of WTTva and rTva were constructed using homology modeling based on the NMR structure of quail Tva. The structures of WTTva and rTva are shown in Figure 5, *A* and *B*, respectively. E53, L55, H59, and G70 were exposed on the surface of WTTva and were spatially adjacent (Fig. 5*A*). The results of homology modeling suggest that the structure of rTva can fold similarly to that of WTTva (Fig. 5*B*). Then the gp85 structure was predicted by the Alphold2 due to the absence of the reported homology structure (Fig. S1 and Table S1), and the molecular details of the interaction between Tva and gp85 were further analyzed. The result of Ligplot+ analysis (28) indicated that these four key residues of Tva (E53, L55, H59, and G70) were distributed on the docking surfaces (Fig. 5, *C* and *D*) and play an

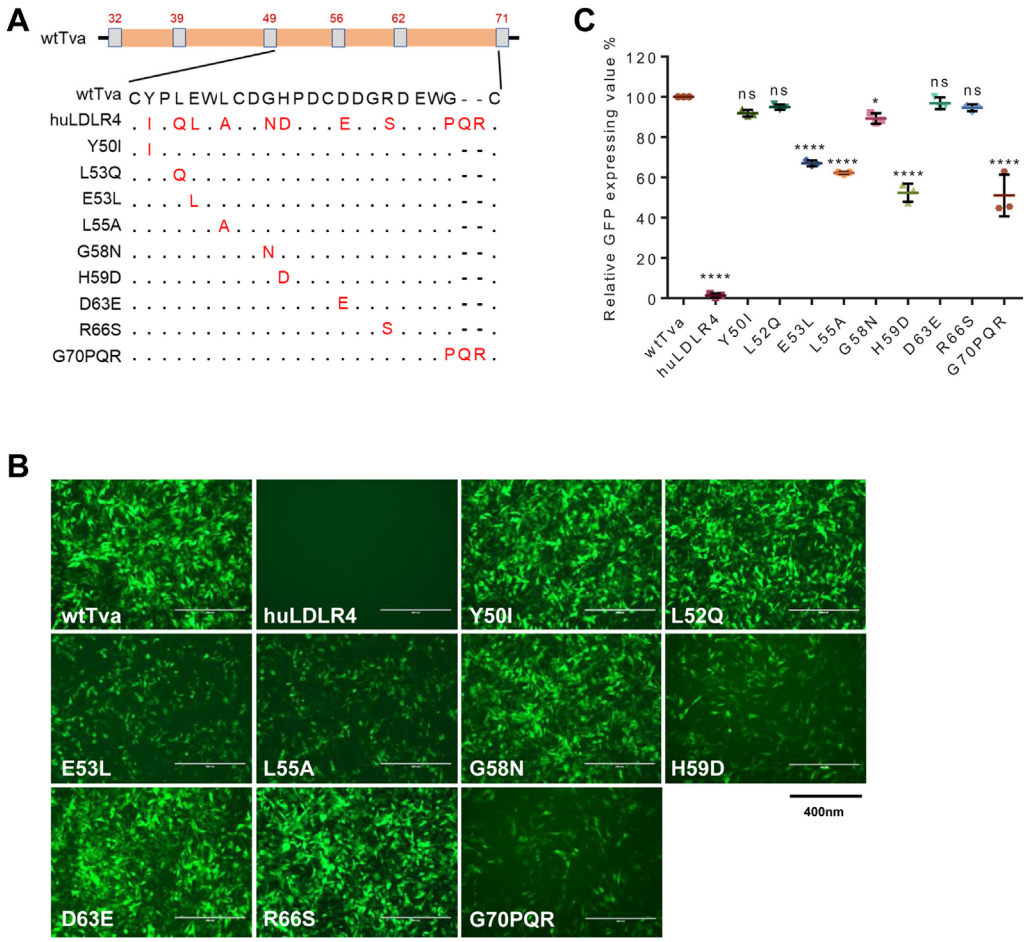

Figure 3. Residues E53, L55, H59, and G70 are key amino acids for Tva mediating virus entry. *A*, schematic representation of the strategy of constructing chimeric receptors with nine different single-residue substitutions. *B*, the entry of RCAS(K)GFP recombinant virus into DF-1-*Tva*KO cells expressing WTTva, huLDLR4, and the nine single-residue substituted chimeric receptors. The fluorescence in WTTva and huLDLR4-transfected cells was used as PC and NC, respectively. The scale bar represents 400 μm. *C*, virus entry levels of the nine single-residue substituted chimeric receptors were detected by flow cytometry. Three independent experiments were performed, and data are shown as means ± SD for triplicates from a representative experiment. *$p < 0.05$; ****$p < 0.0001$; ns, no significant difference. NC, negative control; PC, positive control.

important role in the interaction of Tva and gp85. E53 of Tva interacts with K254 of gp85 forming a salt bridge (5.0 Å), and hydrogen bonds were formed between of G70 of Tva and N171 of gp85 (2.9 Å) as well as H59 of Tva and G207 of gp85 (2.8 Å) (Fig. 5, *E* and *F*). The results showed that the interactions between Tva and gp85 have favorable distances. After substitution of these four residues (Fig. 5*D*), the shape complementarity score showed that the score decreased from 0.409 to 0.301, indicating these mutations were unfavorable to the interaction of Tva with gp85. Furthermore, we calculated the binding free energy of WTTva or rTva binding to gp85 with the generalized born and surface area continuum solvation method. After these four residues were substituted, the binding free energy between Tva and gp85 changed from −24.3504 kcal/mol to 4.9008 kcal/mol (Fig. 5*G*), indicating that the interaction force went from favorable to unfavorable.

These results are consistent with the above results that E53, L55, H59, and G70 directly participate in the interaction between Tva and gp85.

The CT loop of the LDL-A module of tva converts huLDLR4 into a functional receptor for ALV-K

To further explore the roles of E53, L55, H59, and G70 in the receptor function of Tva, a series of chimeric plasmids were constructed based on the backbone of huLDLR4, including five plasmids that substituted L53, A55, D59, or PQR residues into WTTva corresponding residues individually or simultaneously (L53E, A55L, D59H, PQR70G, and hu-ch 4P) and a plasmid (hu-ch CT) that replaced the CT loop of huLDLR4 with that of WTTva (Fig. 6*A*). The virus entry assay showed that L53E, A55L, D59H, and PQR70G failed to mediate virus entry into cells (Fig. 6*B*), showing a less than 5% GFP-positive rate (Fig. 6*C*). Hu-ch 4P acquired the ability to partially mediate RCAS(K)GFP entry into cells (Fig. 6*B*), showing about a 46% GFP-positive rate (Fig. 6*C*). In contrast, hu-ch CT sufficiently mediated RCAS(K)GFP entry into cells (Fig. 6*B*), showing a relative GFP-positive rate of more than 80% (Fig. 6*C*). Co-IP assay results showed that L53E, A55L, D59H, and PQR70G did not interact with gp85, and hu-ch 4P had weak interactions with gp85 (Fig. 6*D*). The ability of hu-ch CT to interact with

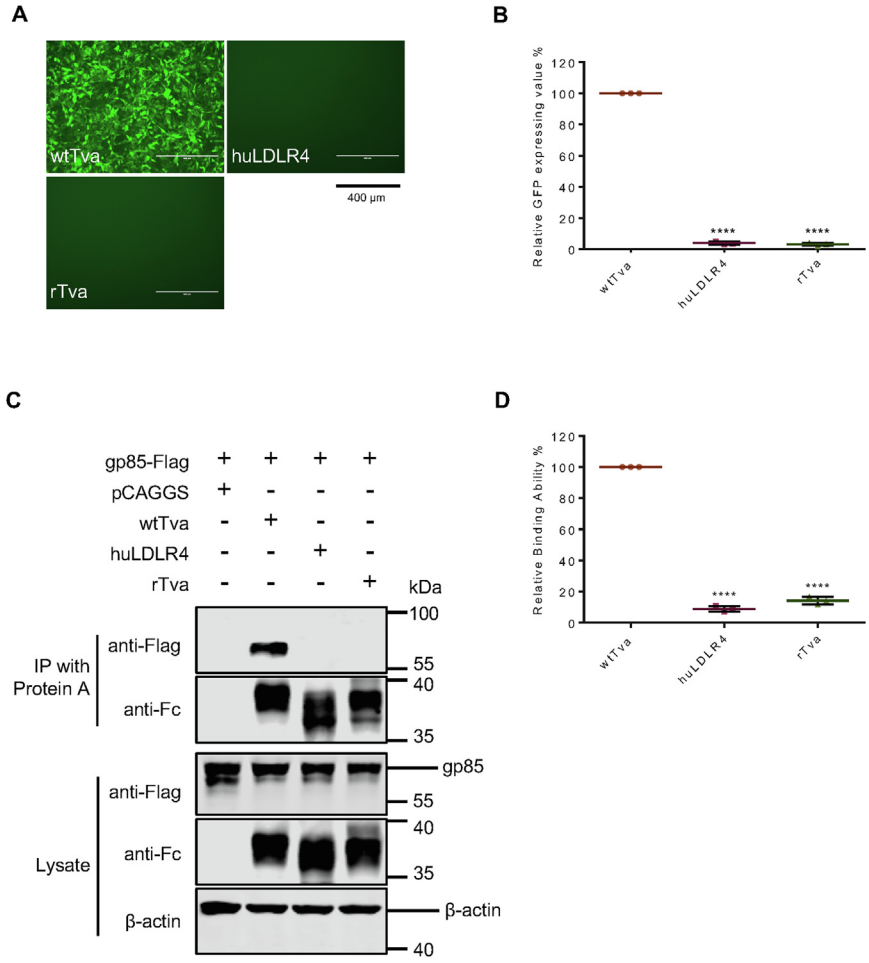

Figure 4. Mutating residues E53, L55, H59, and G70 deprive the receptor function of Tva. *A*, the entry of RCAS(K)GFP recombinant virus into DF-1-*Tva*KO cells expressing rTva. The fluorescence in WTTva and huLDLR4 transfected cells was used as PC and NC, respectively. The scale bar represents 400 μm. *B*, virus entry levels of rTva were detected by flow cytometry. The virus entry-level of WTTva transfected cells was set to 100%, and the values for rTva were calculated as their proportion. *C*, interaction of rTva with gp85 was verified by Co-IP assay. WTTva was used as PC; huLDLR4 was used as NC. *D*, the gp85-binding abilities of rTva expressed on the surface of transfected 293T cells using the protein-cell binding assay. Three independent experiments were performed, and data are shown as means ± SD for triplicates from a representative experiment. ****$p < 0.0001$. Co-IP, Co-immunoprecipitation; NC, negative control; PC, positive control.

gp85 was not significantly different from that of WTTva (Fig. 6*D*). The results of the protein-cell binding assay also showed that, compared with WTTva, the relative binding rates of L53E, A55L, D59H, and PQR70G to gp85 were less than 10% and that for the binding of hu-ch 4P to gp85 was only about 40%. However, the binding ability of hu-ch CT with gp85 was greater than 90% (Fig. 6*E*). These results indicate that although the four residues (E53, L55, H59, and G70) could make huLDLR4 acquire part of the Tva receptor function, the CT loop of the LDL-A module of Tva is the minimal domain for huLDLR4 to acquire the full capacity of Tva.

Gene-edited DF-1 cell lines with E53, L55, H59, and G70 of tva substituted could completely resist ALV-K entry

To investigate whether changing E53, L55, H59, and G70 could render DF-1 cells resistant to ALV-K infection, we constructed a DF-1 cell line (DF-1-rTva) with E53, L55, H59, and G70 mutated into huLDLR4-corresponding residues. Sequence analysis showed that E53, L55, H59, and G70 in DF-1-rTva were successfully replaced by huLDLR4 corresponding residues (Fig. 7*A*). The viability of DF-1-rTva cells was determined using the CCK-8 kit, and the results indicated that substitutions of E53, L55, H59, and G70 did not influence the viability of DF-1-rTva cells (Fig. 7*B*). Cells were infected with RCAS(K)GFP to evaluate the ability of DF-1-rTva cells to resist ALV-K infection. After 72 h, the infected cells were observed, and the results showed that DF-1-rTva cells could completely resist the infection of RCAS(K)GFP (Fig. 7*C*). Flow cytometry analysis also showed that GFP fluorescence could not be detected in DF-1-rTva cells (being lower than 0.3%) (Fig. 7*D*). DF-1-rTva cells were infected with the JS14LH01 strain (WT ALV-K strain). After 7 days, the viral titre was determined. The results showed that the viral titre of ALV-K in WT DF-1 cells was approximately $1 \times 10^{5.57}$ $TCID_{50}$/ml, whereas no viral titre of ALV-K was detected in DF-1-rTva cells, indicating that DF-1-rTva cells could completely resist infection by the JS14LH01 strain (Fig. 7*E*). Studies have indicated that Tva is related to the uptake of transcobalamin-bound vitamin B_{12}/Cbl (29). The ability to internalize

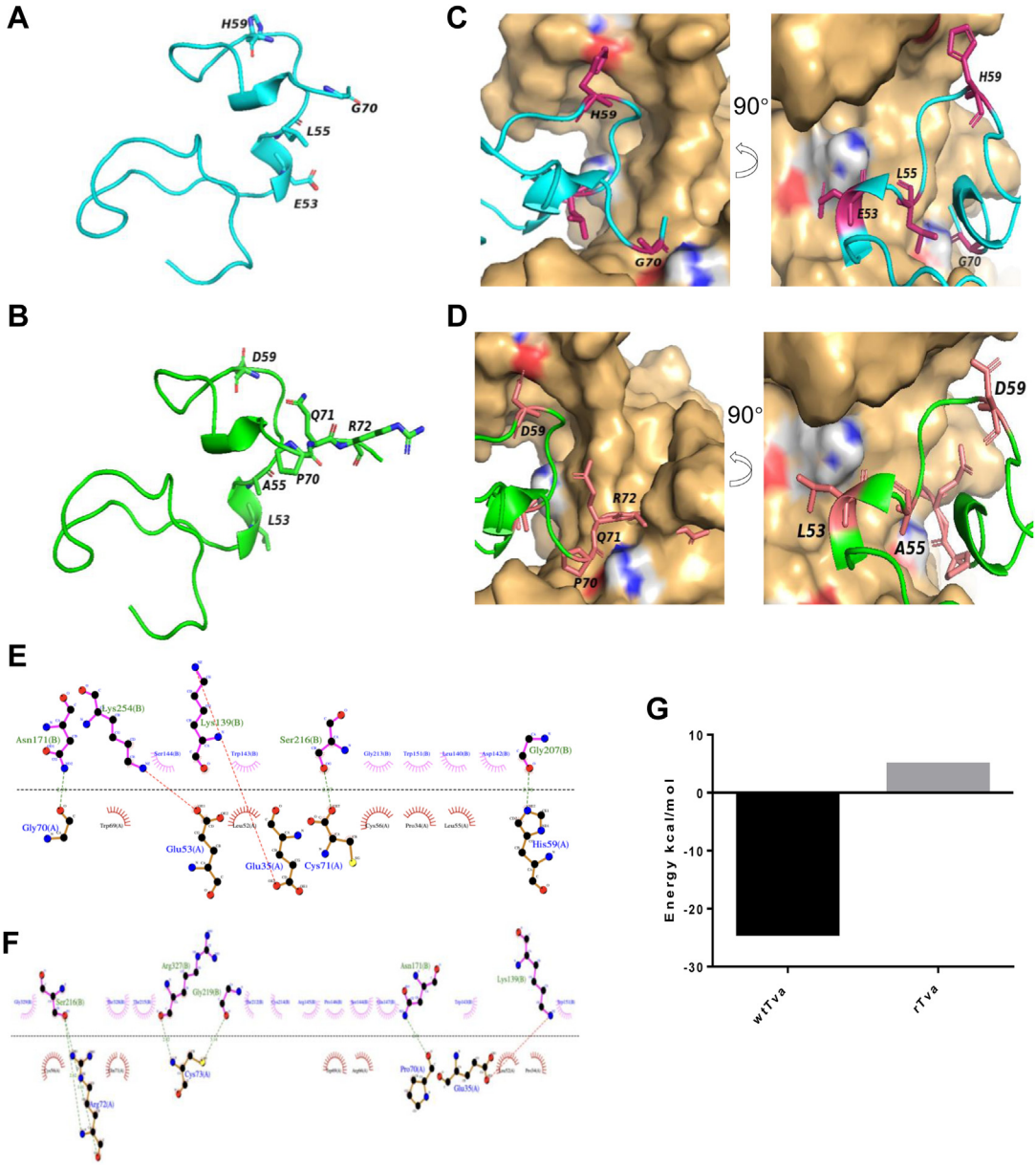

Figure 5. Modeled structure comparison of Tva and rTva LDL-A module and molecular docking of Tva with gp85. *A*, ribbon representation of the modeled structure of the Tva LDL-A module. The side chains of E53, L55, H59, and G70 were displayed. *B*, ribbon representation of the modeled structure of the rTva LDL-A module. The side chains of L53, A55, D59, P70, Q71, and R72 were displayed. *C*, interaction surface of WTTva and gp85. The chain in cyan represents WTTva; the gp85 was in surface representation. The figure at the bottom is the contact surface after 180° rotation. *D*, interaction surface of rTva and gp85. The chain in *green* represents rTva; the gp85 was in surface representation. The figure at the bottom is the contact surface after 180° rotation. *E*, the protein–protein interacting face of Tva with gp85 analyzed by Ligplot+. *F*, the protein–protein interacting face of rTva with gp85 analyzed by Ligplot+. Chain on the upside represents tva; chain on the downside represents gp85; *Green line* and *red line* represent the hydrogen bond and salt bridge, respectively. *G*, binding free energy of WTTva or rTva with gp85.

vitamin B_{12}/Cbl of DF-1-rTva was detected using the confocal assay. The results indicate that DF-1-rTva could efficiently internalize Cbl and showed no obvious difference from WT DF-1. These findings indicate that changing E53, L55, H59, and G70 in Tva makes DF-1 cells completely resistant to the infection of ALV-K without affecting Cbl uptake.

Discussion

ALV-K is a novel subgroup of ALV that was first isolated in China in 2012 (1). ALV-K shares its receptor with ALV-A and uses Tva to enter host cells, the molecular details of which remain unclear. In this study, we demonstrate that the CT loop of the LDL-A module of Tva is the key functional domain for mediating ALV-K entry into host cells. Four amino acid residues (E53, L55, H59, and G70) located on the surface of Tva structures are critical for Tva receptor function. Structural analysis indicated that the binding between Tva and gp85 was almost completely lost after substituting the four residues. In addition, a Tva-modified DF-1 cell line (DF-1-rTva) with E53, L55, H59, and G70 substituted was completely resistant to ALV-K infection. Collectively, our results indicate, for the first

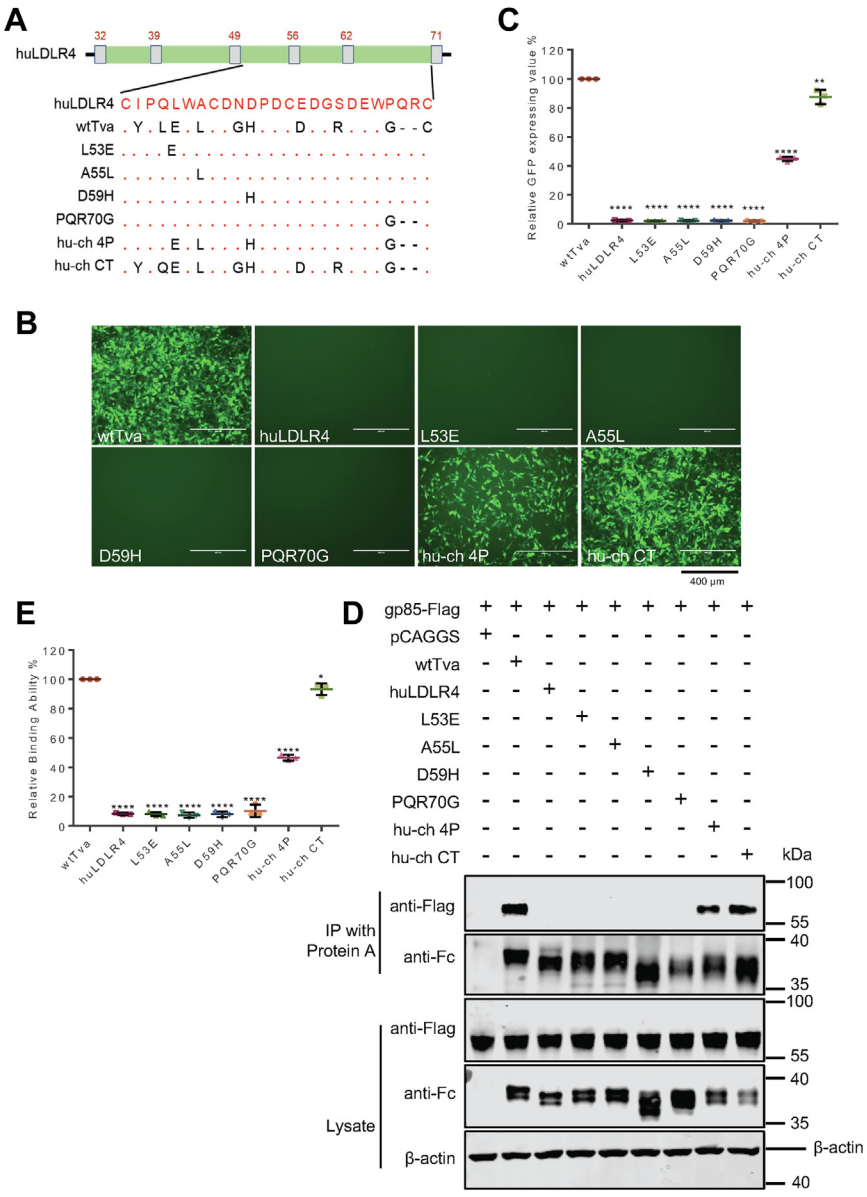

Figure 6. CT loop of the LDL-A module of Tva converts huLDLR4 into a functional receptor for ALV-K. *A*, schematic representation of the strategy of constructing chimeric huLDLR4 receptors with single-residue, four residues, or CT loop substitutions. *B*, entry of RCAS(K)GFP recombinant virus into DF-1-*Tva*KO cells expressing WTTva, huLDLR4, and different huLDLR4 chimeric receptors. The fluorescence in WTTva and huLDLR4 transfected cells was used as PC and NC, respectively. The scale bar represents 400 μm. *C*, virus entry-level of different huLDLR4 chimeric receptors expressing cells were detected by flow cytometry. The entry of WTTva transfected cells was set to 100%, and the values for chimeric huLDLR4 receptors were calculated as their proportion. *D*, Co-IP validation of the interaction of different huLDLR4 chimeric receptors with gp85. WTTva was used as PC; huLDLR4 was used as NC. *E*, the gp85-binding abilities of different huLDLR4 chimeric receptors expressed on the surface of transfected 293T cells using the protein-cell binding assay. Three independent experiments were performed, and data are shown as means ± SD for triplicates from a representative experiment. $^{**}p < 0.01$; $^{****}p < 0.0001$. ALV, avian leukosis virus; Co-IP, Co-immunoprecipitation; CT, C-terminal; NC, negative control; PC, positive control.

time, that E53, L55, H59, and G70 are key residues of Tva that mediate ALV-K entry into host cells.

Tva is a type I transmembrane protein, and its LDL-A module contains two loop structures (NT loop and CT loop), The NT loop has almost no homology among different species, whereas the CT loop shows more than 50% amino acid similarity (11, 30). However, our results show that the CT loop is a key domain of Tva, mediating ALV-K entry into host cells. Structural analysis also showed that Tva only forms an interaction interface with gp85 through the CT loop. Therefore, we speculate that the NT loop of Tva may play a role in maintaining the correct conformation of Tva, rather than in the direct interaction with gp85 and that Tva directly interacts with gp85 through its CT loop to mediate viral entry. These results are consistent with the CT loop of the LDL-A module of Tva responsible for ALV-A entry in quails (31).

Four key residues (E53, L55, H59, and G70) in the CT loop of the LDL-A module of Tva were identified as residues that significantly affected Tva receptor function. However, huLDLR4 only acquired partial Tva receptor function after the simultaneous replacement of these four amino acids, but huLDLR4 fully binds to gp85 and mediates viral entry only by

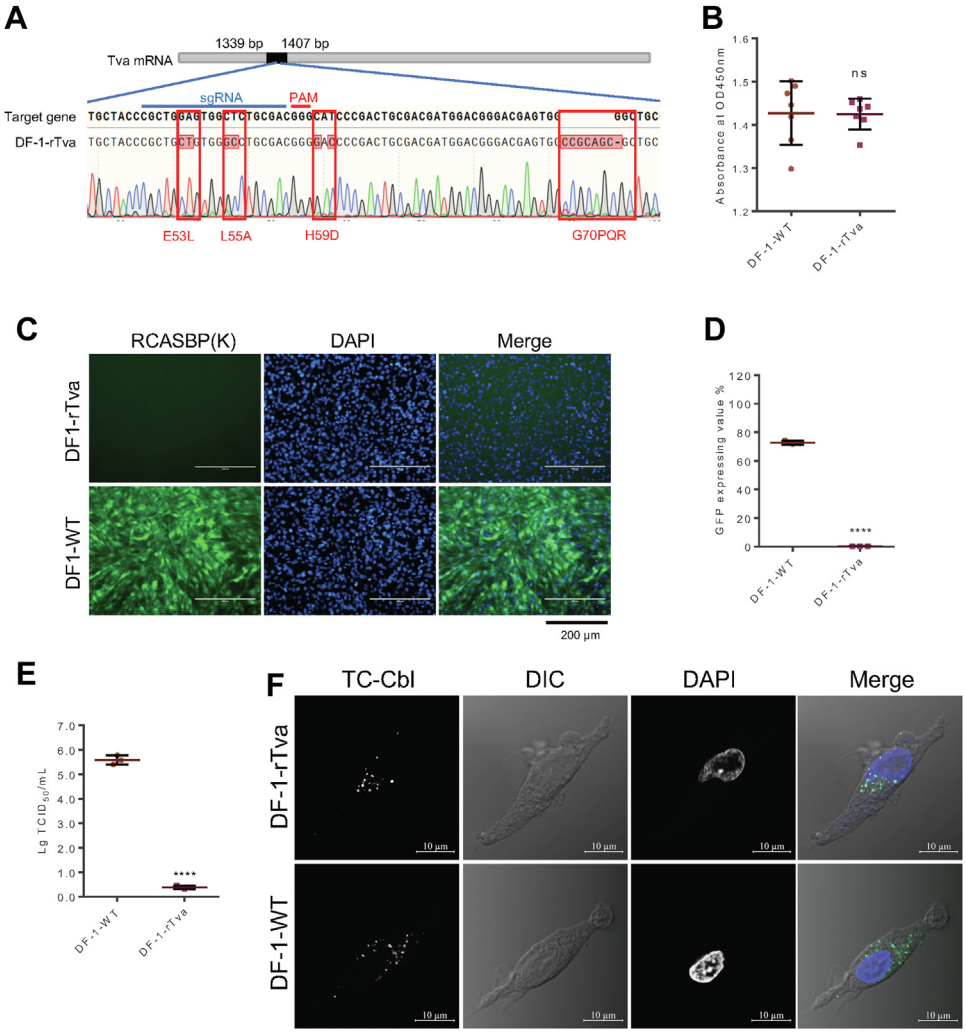

Figure 7. A DF-1 cell line changing E53, L55, H59, and G70 of Tva could completely resist ALV-K entry. *A*, schematic diagram of the construction of Tva gene-edited DF-1 cells and the sequence analysis of DF-1-rTva cell lines. The *red box* indicated the mutant peak of Tva gene. *B*, cell viability of DF-1-WT and DF-1-rTva cell lines. *C*, RCAS(K)GFP infection rate of DF-1-WT or DF-1-rTva cell lines were analyzed at 120 h postinfection under a fluorescence microscope. The scale bar represents 200 μm. *D*, RCAS(K)GFP infection rate of DF-1-WT or DF-1-rTva cell lines and analyzed at 120 h postinfection using flow cytometric. *E*, $TCID_{50}$ in DF-1-WT and DF-1-rTva cell lines were detected 7 days after infection. *F*, confocal analysis of TC-Cbl uptake in DF-1-WT or DF-1-rTva cells. *Green fluorescence* represents TC-Cbl. *Blue fluorescence* represents cell nucleus. Three independent experiments were performed, and data are shown as means ± SD for triplicates from a representative experiment. ****$p < 0.0001$; ns, no significant difference. ALV, avian leukosis virus.

replacing the entire CT loop of the LDL-A module of Tva. Numerous studies have shown that the binding interfaces between proteins rely on multiple intermolecular contacts involving 10 to 30 side chains of each protein (32, 33). Our structural simulation results showed that in addition to the four key amino acids identified in this study, other amino acids of the CT loop are also located on this interaction interface formed by Tva and gp85 and may form weaker contacts between Tva and gp85. To better understand this binding, the role of these amino acids in the interaction between gp85 and Tva should be investigated further.

Viral entry into host cells requires direct interaction between the receptor and virus, but it also requires structural stability of the receptor (30, 34). Structural analysis suggested that E53, L55, H59, and G70 may not play a crucial role in maintaining the structure of Tva but are directly involved in gp85 binding. The protein–protein docking results demonstrated that these key four residues of Tva play an important role to form polar bonds between Tva and gp85. Furthermore, after these four residues of Tva mutated, both the shape complementary results and the free energy calculation results indicate that mutation of these residues decreased the ability for Tva binding to the gp85. In addition, these four amino acids could enable huLDLR4 to partially interact with gp85, which means that these residues are involved in mediating viral entry by affecting the direct interaction between Tva and gp85.

In recent years, gene-editing technology has been widely used in disease resistance breeding, for which receptors are the best gene-editing targets (35). For example, the porcine reproductive and respiratory syndrome virus receptor CD163 or the transmissible gastroenteritis virus receptor *pAPN* gene knockout pigs could completely resist porcine reproductive and respiratory syndrome virus or the transmissible gastroenteritis virus infection (36, 37). However, some receptors are involved in regulating various signaling pathways in host cells.

The ALV-J receptor, chNHE1, is involved in basic cellular functions, including cell adhesion and manipulation of the extracellular pH (38, 39). The foot-and-mouth disease virus receptor is integrin αvβ3, which plays an important role in cell growth and differentiation (40, 41). Therefore, precise editing of key sites of cell receptors can not only resist virus infection but will also not affect the physiological function of the receptor protein, which will be an important direction of antiviral research in the future. Tva is involved in TC-mediated Cbl uptake (29). Although Tva-deficient gene-edited chickens have been generated and could completely resist ALV-K infection, they exhibit specific Cbl metabolic disturbances due to the lack of Tva (42). In this study, E53, L55, H59, and G70 were identified as the key residues for Tva to interact with gp85 and mediate ALV-K entry into host cells. Furthermore, we found that the Tva gene-edited DF-1 cell line with E53L, L55A, H59D, and G70PQR precise mutations did not affect the activity of DF-1 cells and their uptake of vitamin B_{12}/Cbl, but completely inhibited the infection of ALV-K. These results further demonstrate that *in vivo* E53, L55, H59, and G70 are the key functional amino acid residues of Tva. These findings provide specific gene-editing target sites for constructing chickens resistant to ALV-K infection. They also provide a theoretical basis for studying disease resistance breeding for other viruses.

Experimental procedures

Cells culture and virus

293T cells or DF-1 cells were grown in Dulbecco's modified Eagle's medium (DMEM) (L110KJ, BasalMedia), supplemented with 10% fetal bovine serum (FBS) (FDN500, Excell Bio), and 1% Penicillin-Streptomycin, incubating in an incubator with 5% CO_2 at 37 °C or 38.5 °C. 293F cells were maintained in serum-free DMEM (H310KJ, BasalMedia) in the presence of 5% CO_2 at 37 °C. The ALV-K strain JS14LH01 (Accession number: MT624731) (4) was stored by our laboratory, and the RCAS(K)GFP (ALV-K enveloped replication-competent avian leukosis sarcoma virus harboring an eGFP reporter gene) recombinant virus was constructed as previously described (19) and stored by our laboratory.

Expression of soluble gp85 protein

The eukaryotic expression plasmid of soluble gp85 was constructed as described previously (18). Briefly, the gp85-encoding gene of JS14LH01 was amplified from the proviral DNA and fused with a signal peptide in the NT and a constant region fragment of human IgG (gp85-Fc) or a Flag tag (gp85-Flag) in the CT by overlapping PCR. Then the gp85-Fc and gp85-Flag were cloned into the pCAGGS vector to generate pCA-gp85-Fc and pCA-gp85-Flag plasmids, respectively. Then, the pCA-gp85-Fc plasmid was transfected into 293F cells using Polyethyleneimine Linear MW40000 (49,533–93–7, Yeasen) for protein purification. At 4 days post-transfection, the cell culture medium was collected and purified using protein A affinity matrix beads (L00210, Genscript) by following the manufacturer's instructions. The concentration of gp85 was determined using the bicinchoninic acid protein assay kit (P0012, Beyotime).

Construction of various chimeric receptors

The WTTva encoding gene was amplified from the cDNA of DF-1 cells using specific primers based on the published chicken *Tva* sequence (Accession number: NC_052600). The human LDLR4 (huLDLR4) encoding gene (Accession number: NM_000527) was synthesized by Sino Biological Inc. Both genes were fused with a signal peptide sequence, a transmembrane domain, and a Flag tag and cloned into the eukaryotic expression vector pCAGGS.

Based on the WTTva backbone, two chimeric receptors with the N- or CT loop domain replaced by the corresponding domain of huLDLR4 were constructed by overlapping PCR. Furthermore, the CT loop of WTTva was divided into three segments (L1, L2, and L3), and they were replaced by the corresponding domains of huLDLR4 by overlapping PCR, respectively.

To map the key residues responsible for Tva mediating ALV-K entry into host cells, a series of WTTva or huLDLR4 point mutational chimeric receptors were generated by replacing the corresponding amino acid coding sequence with overlapping PCR.

Furthermore, the soluble form of WTTva, huLDLR4, and different chimeric receptors contained a signal peptide sequence at the NT and the Fc region of a human IgG at the CT, and a cytoplasmic domain with a hemagglutinin tag was constructed by overlapping PCR and inserted into a pCAGGS vector.

Confocal assays

To visualize the expression of WTTva, huLDLR4, ch-hu NT, and ch-hu CT proteins on cell surface, TvaKO DF-1 cells were transfected with plasmids encoding WTTva, huLDLR4, ch-hu NT, and ch-hu CT. After 24 h, cells were washed by PBS three times, fixed by 4% (vol/vol) paraformaldehyde (PFA) for 15 min at room temperature (RT), and blocked by 5% (wt/vol) skim milk in PBS for 1 h at RT. The cells were incubated with anti-flag monoclonal antibody (mAb) produced in mice (F1804, SLCD6338, Sigma-Aldrich) for 1 h at RT. Washing three times with PBS, the cells were incubated with anti-mice IgG (whole molecule)-tetramethyl rhodamine isocyanate (TRITC) antibody produced in rabbit (T2402, 092M4751V, Sigma-Aldrich) for 1 h at RT. Then, the cells were washed three times with PBS and staining with 4′,6-diamidino-2-phenylindole (C1005, Beyotime) for 15 min. Finally, the cells were examined using a Lecia SP2 confocal system (Lecia Microsystems).

Viral entry assay

The viral entry assay was performed with the RCAS(K)GFP virus to evaluate the ability of WTTva, huLDLR4, and different chimeric receptors to mediate ALV-K entry into host cells. DF-1-TvaKO cells were transfected with plasmids encoding WTTva, huLDLR4, or different chimeric receptors. After 24 h,

ASBMB

transfected DF-1-TvaKO cells were infected with RCAS(K) GFP virus at a multiplicity of infection of 0.1. After 2 h at 37 °C and 5% CO_2 (*i.e.*, conditions allowing efficient viral entry), the cells were washed three times with RT PBS and maintained in DMEM containing 2% (wt/vol) FBS at 38.5 °C with 5% CO_2. At 72 h postinfection, the cells were observed under fluorescence microscopy. Then, the cells were digested by trypsin and firstly strained by anti-flag mAb produced in mice (F1804, SLCD6338, Sigma-Aldrich) and secondly strained by the anti-mice IgG (whole molecule) TRITC antibody produced in rabbit (T2402, 092M4751V, Sigma-Aldrich). The stained cells were analyzed using a FACS Aria II flow cytometer (Cytomics TM FC 500, BD Biosciences). The virus entry-level of DF-1-TvaKO cells expressing WTTva was set as 100%, and the values for other receptors were calculated as its proportion. All the samples were prepared independently at least three times for three independent experiments.

Co-IP assay

293T cells were transfected with the respective plasmids using Polyjet (SL100688, SignaGen Laboratories), according to the manufacturer's instructions. After 48 h, the transfected 293T cells were washed three times with ice-cold PBS and then lysed in NP-40 cell lysis buffer (P0013F, Beyotime Biotech Inc). After centrifugation, 40 μl of the supernatant was collected as the input fraction. The remaining supernatant was collected as the Co-IP fraction, and it was incubated with protein A resin at 4 °C for 6-8 h. Then the protein A affinity matrix beads were collected by centrifugation at 1000*g* for 5 min at 4 °C and washed five times with ice-cold PBS. The immunoprecipitated proteins were separated by SDS-PAGE and detected by Western blotting. All the experiments were performed with three biological replicates.

Western blotting

Proteins were separated by 10% SDS-PAGE gels and transferred onto a nitrocellulose membrane (HATF00010, Merck-Millipore). After blocking with 5% (wt/vol) skimmed milk for 2 h, membranes were incubated with anti-flag mAb (F1804, SLCD6338, Sigma-Aldrich) produced in mice for 1 h at RT. Followed y washing it three times with PBS, containing 0.05% Tween 20. Then, the membranes were incubated with IRDye 800CW goat anti-mice IgG (926–32212, D20427–25, LI-COR Biosciences) and goat anti-human IgG (Fc-specific) antibodies (925–32232, C50326–05, LI-COR Biosciences) for 1 h at RT. Finally, the membrane blots were scanned using an Odyssey infrared imaging system (LI-COR Biosciences).

Protein-cell binding assay

Plasmids encoding WTTva, huLDLR4, or different chimeric receptors were used to transfect 293T cells. The transfected cells were digested by trypsin, centrifuged for 5 min (1000*g*), and washed with ice-cold PBS containing 5% (wt/vol) FBS. Then, 293T cells were incubated with 500 μl gp85 proteins (200 ng/μl) for 1 h on ice and stained with a 1:200 dilution of anti-human IgG (Fc-specific)-FITC antibody produced in goat (F9512, SLCC5427, Sigma-Aldrich). Then, the cells were fixed in 4% (vol/vol) PFA (P1110, Solarbio) for 15 min at RT. Finally, the cells were incubated with a 1:200 dilution of monoclonal anti-flag mAb produced in mice for 1 h on ice, followed by staining with a 1:200 dilution of anti-mice IgG (whole molecule) TRITC antibody (T2402, 092M4751V, Sigma-Aldrich). Stained cells were analyzed using an FACS Aria II flow cytometer (Cytomics TM FC 500, BD Biosciences). Cells transfected with WTTva were set as 100%, and the values for other receptors were calculated as their proportion. All the samples were prepared independently at least three times for three independent experiments.

Structure analysis

The models were built using the Modeller 10.2 server (43). We got the WTTva structure by using the Modeller 10.2 server based on the NMR structure of quail Tva (PDB code: 1k7b). The rTva structure was got by using mutagenesis wizard of PyMOL based on the optimized structure of WTTva. Furthermore, the WTTva and rTva structures were optimized with MD simulation for 200 ns through amber 20. The gp85 structure was predicted by Alphold2 (44, 45). These models were optimized by dynamic simulation using Amber 20. Following, we carried out the WTTva-gp85 docking model using the hdock server (46) (http://hdock.phys.hust.edu.cn/);then the highest-scoring model was chosen as the initial docking model and optimized in the ROSETTA2020 software (47) to obtain the final WTTva-gp85 docking results for further interaction analysis. Next, we used the optimized rTva to replace the WTTva in the final WTTva-gp85 docking model to obtain the final rTva-gp85 complex model. Finally, the final rTva-gp85 complex model and WTTva-gp85 complex mode were selected for further interaction analysis. The shape complementarity was analyzed by using the InterfaceAnalyzer module (48). The protein–protein interaction face was analyzed by Ligplot+ (28). The binding free energy of WTTva or rTva with gp85 was calculated by the generalized born and surface area continuum solvation method based on the final docking results.

MD simulation

TIP3P water model was employed to build the water box and added some chlorine or sodium ions to neutralize the system. AMBER20 package (46) was employed to run the MD simulations with leaprc.protein.ff14SB (49) as the force field for the protein. Firstly, we performed energy minimization to obtain a low energy starting conformation for the subsequent MD simulations. Four thousand steps of steepest descent method were initially employed, followed by six thousand steps of conjugate gradient method. The whole system was minimized, followed by minimization of the solutes, protein and ligand. With the Langevin thermostat applied, the system was heated under canonical ensemble from 0 to 310 K for 300 ps, with the force constant for the harmonic restraint set to be 10.0 kcal mol−1Å − 2. The system was then equilibrated

for 10 ns under isothermal–isobaric ensemble (constant pressure = 1.0 bar). The relaxation time for barostat bath was 2.0 ps. Finally, the production simulation was run for 200 ns under isothermal–isobaric ensemble with periodic boundary conditions. The time step was set to be 2 fs and bonds connected with hydrogen atoms were constrained using the SHAKE algorithm. The long-range electrostatics was handled by the particle mesh Ewald method (50). The cut-off value for short range interactions was set to be 8.0 Å. The cpptraj (51) tool in AMBER 20 was applied to calculate the root mean square deviation of the calcium atoms to analyze the stability of the complexes during the simulation; 336 Cα atoms of gp85 or 40 Cα atoms of Tva were included in the calculation, respectively.

Tva-modified DF-1 (DF-1-rTva) cell line construction

DF-1-rTva cell lines were constructed using CRISPR/Cas9 technology. Firstly, the gRNA-targeting *Tva* sites (CGCTGG AGTGGCTCTGCGAC) were designed by E-CRISP. Next, the DNA fragments containing the U6 promoter, targeted RNA sites, and gRNA scaffold were fused and inserted into the pMD18-T vector (6011, TAKARA BIO INC). The plasmid was extracted by the QIAfilter Plasmid Midi Kit (12,245, Qiagen). Moreover, we have designed and synthesized a single-stranded oligodeoxynucleotide containing four amino acid residues mutation (E53L, L55A, H59D, and G70PQR) as the template for homologous recombination.

To construct DF-1-rTva cells, DF-1-WT cells were cotransfected with 2 μg pMJ920 (Addegene: #42234) plasmid, a 2 μg plasmid containing gRNA and 10 μl single-stranded oligodeoxynucleotide (10 μM) using the Mirus X-2 (MIR 6000, Mirusbio), according to the manufacturer's instructions. 48 h post-transfection, the cells with green fluorescence were screened by flow cytometry and put into 96-well plates with serial dilutions to obtain a single-cell colony. After about 15 days, the genomic DNA of monoclonal DF-1 cells were extracted, and PCR amplified its *Tva*-encoding gene. Finally, it was determined by sequencing.

Cell viability assay

DF-1-WT and DF-1-rTva cells were put into 96-well plates with 4×10^4 density. Cells were cultured for 6 to 8 h and added 10 μl CCK-8 solution (CK04, Dojindo Laboratories) per well. After mixing, the absorbance of cells at 450 nm was measured with a microplate reader at 2 h after incubation. The experiment was repeated at least three times.

Viral titer determination

The infected cell supernatants were harvested at 7 days postinfection. The titers of supernatants were determined in 50% tissue infection dose ($TCID_{50}$)/ml by using the Reed–Muench method. Three independent experiments were performed.

TC-Cbl uptake assay

After DF-1-WT cells and DF-1-rTva cells were seeded on microscope cover glasses and maintained for 24 h, they were incubated with TC-Cbl (29) at 37 °C for 1 h. Then the cells were washed with PBS and fixed with 4% PFA. Further, the cells were stained with 4′,6-diamidino-2-phenylindole (C0065–50, Solarbio) for 10 min and examined by a laser confocal microscope (LSM980, ZEISS). The experiments were performed with three biological replicates.

Statistical analysis

All assays were performed independently with samples prepared for at least three times and carried out corresponding experiments to achieve the purpose of three biological replicates. Prism software (Version 7.03) was employed for statistical analyzes, and the Student's *t*-tests were performed to establish differences between groups. Statistical significance was set at $p < 0.05$.

Data availability

All data generated are contained within the article and supporting information.

Supporting information—This article contains supporting information (44, 45).

Acknowledgments—This work was supported by the National Natural Science Foundation of China (32230105 and 31872482), Heilongjiang Touyan Innovation Team Program, and China's Agricultural Research System (CARS-41).

Author contributions—X. L., Y. C., and Y. G. conceptualization; X. Q., K. L., L. G., Y. Z., C. L., H. C., and X. W. resources; X. L., Y. C., M. Y., S. W., and Y. G. data curation; Y. G. formal analysis; X. L., Y. C., and Y. G. supervision; Y. G. funding acquisition; X. L., Y. C., M. Y., S. W., and Y. G. validation; X. L., Y. C., M. Y., S. W., P. L., L. M., R. G., X. F., M. H., T. H., X. Q., K. L., L. G., Y. Z., C. L., H. C., X. W., and Y. G. investigation; X. L., Y. C., and Y. G. writing – original draft; Y. G. project administration; X. L., Y. C., and Y. G. writing – review and editing.

Conflict of interest—The authors declare that they have no conflicts of interest with the contents of this article.

Abbreviations—The abbreviations used are: ALV, avian leukosis virus; Co-IP, Co-immunoprecipitation; Env, envelope; FBS, fetal bovine serum; FeLV-B, feline leukaemia virus subgroup B; FeLV-T, T-cell-tropic FeLV; mAb, monoclonal antibody; PFA, paraformaldehyde; TRITC, tetramethyl rhodamine isocyanate.

References

1. Cui, N., Su, S., Chen, Z., Zhao, X., and Cui, Z. (2014) Genomic sequence analysis and biological characteristics of a rescued clone of avian leukosis virus strain JS11C1, isolated from indigenous chickens. *J. Gen. Virol.* **95**, 2512–2522
2. Zhao, Z., Rao, M., Liao, M., and Cao, W. (2018) Phylogenetic analysis and pathogenicity assessment of the emerging recombinant subgroup K of

avian leukosis virus in South China. *Viruses* **10**. https://doi.org/10.3390/v10040194
3. Ochi, A., Ochiai, K., Kobara, A., Nakamura, S., Hatai, H., Handharyani, E., *et al.* (2012) Epidemiological study of fowl glioma-inducing virus in chickens in Asia and Germany. *Avian Pathol.* **41**, 299–309
4. Li, X., Yu, Y., Ma, M., Chang, F., Muhammad, F., Yu, M., *et al.* (2021) Molecular characteristic and pathogenicity analysis of a novel multiple recombinant ALV-K strain. *Vet. Microbiol.* **260**, 109184. https://doi.org/10.1016/j.vetmic.2021.109184
5. Liang, X., Gu, Y., Chen, X., Li, T., Gao, Y., Wang, X., *et al.* (2019) Identification and characterization of a novel natural recombinant avian leucosis virus from Chinese indigenous chicken flock. *Virus genes* **55**, 726–733
6. Su, Q., Li, Y., Cui, Z., Chang, S., and Zhao, P. (2018) The emerging novel avian leukosis virus with mutations in the pol gene shows competitive replication advantages both *in vivo* and *in vitro*. *Emerg. Microbes Infect.* **7**, 117
7. Mothes, W., Boerger, A. L., Narayan, S., Cunningham, J. M., and Young, J. A. (2000) Retroviral entry mediated by receptor priming and low pH triggering of an envelope glycoprotein. *Cell* **103**, 679–689
8. Barnard, R. J., Elleder, D., and Young, J. A. (2006) Avian sarcoma and leukosis virus-receptor interactions: from classical genetics to novel insights into virus-cell membrane fusion. *Virology* **344**, 25–29
9. Battini, J. L., Danos, O., and Heard, J. M. (1998) Definition of a 14-amino-acid peptide essential for the interaction between the murine leukemia virus amphotropic envelope glycoprotein and its receptor. *J. Virol.* **72**, 428–435
10. Zhang, B., Sun, C., Jin, S., Cascio, M., and Montelaro, R. C. (2008) Mapping of equine lentivirus receptor 1 residues critical for equine infectious anemia virus envelope binding. *J. Virol.* **82**, 1204–1213
11. Bates, P., Young, J. A., and Varmus, H. E. (1993) A receptor for subgroup A Rous sarcoma virus is related to the low density lipoprotein receptor. *Cell* **74**, 1043–1051
12. Young, J. A., Bates, P., and Varmus, H. E. (1993) Isolation of a chicken gene that confers susceptibility to infection by subgroup A avian leukosis and sarcoma viruses. *J. Virol.* **67**, 1811–1816
13. Adkins, H. B., Brojatsch, J., Naughton, J., Rolls, M. M., Pesola, J. M., and Young, J. A. (1997) Identification of a cellular receptor for subgroup E avian leukosis virus. *Proc. Natl. Acad. Sci. U. S. A.* **94**, 11617–11622
14. Adkins, H. B., Blacklow, S. C., and Young, J. A. (2001) Two functionally distinct forms of a retroviral receptor explain the nonreciprocal receptor interference among subgroups B, D, and E avian leukosis viruses. *J. Virol.* **75**, 3520–3526
15. Elleder, D., Plachý, J., Hejnar, J., Geryk, J., and Svoboda, J. (2004) Close linkage of genes encoding receptors for subgroups A and C of avian sarcoma/leucosis virus on chicken chromosome 28. *Anim. Genet.* **35**, 176–181
16. Elleder, D., Stepanets, V., Melder, D. C., Senigl, F., Geryk, J., Pajer, P., *et al.* (2005) The receptor for the subgroup C avian sarcoma and leukosis viruses, Tvc, is related to mammalian butyrophilins, members of the immunoglobulin superfamily. *J. Virol.* **79**, 10408–10419
17. Chai, N., and Bates, P. (2006) Na+/H+ exchanger type 1 is a receptor for pathogenic subgroup J avian leukosis virus. *Proc. Natl. Acad. Sci. U. S. A.* **103**, 5531–5536
18. Guan, X., Zhang, Y., Yu, M., Ren, C., Gao, Y., Yun, B., *et al.* (2018) Residues 28 to 39 of the extracellular loop 1 of chicken Na^+/H^+ exchanger type I mediate cell binding and entry of subgroup J avian leukosis virus. *J. Virol.* **92**, e01627-17
19. Přikryl, D., Plachý, J., Kučerová, D., Koslová, A., Reinišová, M., Šenigl, F., *et al.* (2019) The novel avian leukosis virus subgroup K shares its cellular receptor with subgroup A. *J. Virol.* **93**, e00580-19
20. Xing, L., Yu, Y., Yu, M., Chang, F., Bao, Y., Wang, S., *et al.* (2020) Identification of cellular receptor mediating subgroup K avian leukosis virus binding and entry its host cell. *Chin. J. Prev. Vet. Med.* **42**, 802–808
21. Lauring, A. S., Cheng, H. H., Eiden, M. V., and Overbaugh, J. (2002) Genetic and biochemical analyses of receptor and cofactor determinants for T-cell-tropic feline leukemia virus infection. *J. Virol.* **76**, 8069–8078
22. Dreyer, K., Pedersen, F. S., and Pedersen, L. (2000) A 13-amino-acid Pit1-specific loop 4 sequence confers feline leukemia virus subgroup B receptor function upon Pit2. *J. Virol.* **74**, 2926–2929
23. Knauss, D. J., and Young, J. A. (2002) A fifteen-amino-acid TVB peptide serves as a minimal soluble receptor for subgroup B avian leukosis and sarcoma viruses. *J. Virol.* **76**, 5404–5410
24. Klucking, S., and Young, J. A. (2004) Amino acid residues Tyr-67, Asn-72, and Asp-73 of the TVB receptor are important for subgroup E avian sarcoma and leukosis virus interaction. *Virology* **318**, 371–380
25. Rong, L., and Bates, P. (1995) Analysis of the subgroup A avian sarcoma and leukosis virus receptor: the 40-residue, cysteine-rich, low-density lipoprotein receptor repeat motif of tva is sufficient to mediate viral entry. *J. Virol.* **69**, 4847–4853
26. Clark, L. E., Clark, S. A., Lin, C., Liu, J., Coscia, A., Nabel, K. G., *et al.* (2022) VLDLR and ApoER2 are receptors for multiple alphaviruses. *Nature* **602**, 475–480
27. Zhang, Y., Yu, M., Xing, L., Liu, P., Chen, Y., Chang, F., *et al.* (2020) The bipartite sequence motif in the N and C termini of gp85 of subgroup J avian leukosis virus plays a crucial role in receptor binding and viral entry. *J. Virol.* **94**, e01232-20
28. Laskowski, R. A., and Swindells, M. B. (2011) LigPlot+: multiple ligand-protein interaction diagrams for drug discovery. *J. Chem. Inf. Model.* **51**, 2778–2786
29. Krchlíková, V., Mikešová, J., Geryk, J., Bařinka, C., Nexo, E., Fedosov, S. N., *et al.* (2021) The avian retroviral receptor Tva mediates the uptake of transcobalamin bound vitamin B_{12} (cobalamin). *J. Virol.* **95**, e02136-20
30. Wang, Q. Y., Manicassamy, B., Yu, X., Dolmer, K., Gettins, P. G., and Rong, L. (2002) Characterization of the LDL-A module mutants of Tva, the subgroup A Rous sarcoma virus receptor, and the implications in protein folding. *Protein Sci.* **11**, 2596–2605
31. Zingler, K., Bélanger, C., Peters, R., Agard, E., and Young, J. A. (1995) Identification and characterization of the viral interaction determinant of the subgroup A avian leukosis virus receptor. *J. Virol.* **69**, 4261–4266
32. Lo Conte, L., Chothia, C., and Janin, J. (1999) The atomic structure of protein-protein recognition sites. *J. Mol. Biol.* **285**, 2177–2198
33. Clark, A. J., Gindin, T., Zhang, B., Wang, L., Abel, R., Murret, C. S., *et al.* (2017) Free energy perturbation calculation of relative binding free energy between broadly neutralizing antibodies and the gp120 glycoprotein of HIV-1. *J. Mol. Biol.* **429**, 930–947
34. Blacklow, S. C., and Kim, P. S. (1996) Protein folding and calcium binding defects arising from familial hypercholesterolemia mutations of the LDL receptor. *Nat. Struct. Biol.* **3**, 758–762
35. Hirakawa, M. P., Krishnakumar, R., Timlin, J. A., Carney, J. P., and Butler, K. S. (2020) Gene editing and CRISPR in the clinic: current and future perspectives. *Biosci. Rep.* **40**. https://doi.org/10.1042/bsr20200127
36. Whitworth, K. M., Rowland, R. R., Ewen, C. L., Trible, B. R., Kerrigan, M. A., Cino-Ozuna, A. G., *et al.* (2016) Gene-edited pigs are protected from porcine reproductive and respiratory syndrome virus. *Nat. Biotechnol.* **34**, 20–22
37. Xu, K., Zhou, Y., Mu, Y., Liu, Z., Hou, S., Xiong, Y., *et al.* (2020) CD163 and pAPN double-knockout pigs are resistant to PRRSV and TGEV and exhibit decreased susceptibility to PDCoV while maintaining normal production performance. *eLife* **9**, e57132. https://doi.org/10.7554/eLife.57132
38. Bhartur, S. G., Ballarin, L. J., Musch, M. W., Bookstein, C., Chang, E. B., and Rao, M. C. (1999) A unique Na+/H+ exchanger, analogous to NHE1, in the chicken embryonic fibroblast. *Am. J. Physiol.* **276**, R838–846
39. Gupta, A., Edwards, J. C., and Hruska, K. A. (1996) Cellular distribution and regulation of NHE-1 isoform of the NA-H exchanger in the avian osteoclast. *Bone* **18**, 87–95
40. Cruet-Hennequart, S., Maubant, S., Luis, J., Gauduchon, P., Staedel, C., and Dedhar, S. (2003) alpha(v) integrins regulate cell proliferation through integrin-linked kinase (ILK) in ovarian cancer cells. *Oncogene* **22**, 1688–1702
41. Meerovitch, K., Bergeron, F., Leblond, L., Grouix, B., Poirier, C., Bubenik, M., *et al.* (2003) A novel RGD antagonist that targets both alphavbeta3 and alpha5beta1 induces apoptosis of angiogenic endothelial cells on type I collagen. *Vascul. Pharmacol.* **40**, 77–89

42. Koslová, A., Trefil, P., Mucksová, J., Krchlíková, V., Plachý, J., Krijt, J., *et al.* (2021) Knock-out of retrovirus receptor gene tva in the chicken confers resistance to avian leukosis virus subgroups A and K and affects cobalamin (vitamin B_{12})-dependent level of methylmalonic acid. *Viruses* **13**, 2504
43. Webb, B., and Sali, A. (2016) Comparative protein structure modeling using MODELLER. *Curr. Protoc. Bioinform.* **54**. https://doi.org/10.1002/cpbi.3
44. Jumper, J., Evans, R., Pritzel, A., Green, T., Figurnov, M., Ronneberger, O., *et al.* (2021) Highly accurate protein structure prediction with AlphaFold. *Nature* **596**, 583–589
45. Bryant, P., Pozzati, G., and Elofsson, A. (2022) Improved prediction of protein-protein interactions using AlphaFold2. *Nat. Commun.* **13**, 1265
46. Lee, T. S., Allen, B. K., Giese, T. J., Guo, Z., Li, P., Lin, C., *et al.* (2020) Alchemical binding free energy calculations in AMBER20: advances and best practices for drug discovery. *J. Chem. Theor. Comput.* **60**, 5595–5623
47. Gray, J. J., Moughon, S., Wang, C., Schueler-Furman, O., Kuhlman, B., Rohl, C. A., *et al.* (2003) Protein-protein docking with simultaneous optimization of rigid-body displacement and side-chain conformations. *J. Mol. Biol.* **331**, 281–299
48. Stranges, P. B., and Kuhlman, B. (2013) A comparison of successful and failed protein interface designs highlights the challenges of designing buried hydrogen bonds. *Protein Sci.* **22**, 74–82
49. Maier, J. A., Martinez, C., Kasavajhala, K., Wickstrom, L., Hauser, K. E., and Simmerling, C. (2015) ff14SB: improving the accuracy of protein side chain and backbone parameters from ff99SB. *J. Chem. Theor. Comput.* **11**, 3696–3713
50. Darden, T., York, D. M., and Pedersen, L. G. (1993) Particle mesh Ewald: an N·log(N) method for Ewald sums in large systems. *J. Chem. Phys.* **98**, 10089–10092
51. Roe, D. R., and Cheatham, T. E., 3rd (2013) PTRAJ and CPPTRAJ: software for processing and analysis of molecular dynamics trajectory data. *J. Chem. Theor. Comput.* **9**, 3084–3095